SF2A 2012
S. Boissier, P. de Laverny, N. Nardetto, R. Samadi, D. Valls-Gabaud and H. Wozniak (eds)

IMPACT OF NON-LTE EFFECTS ON THE IR CA II TRIPLET AND THE MG I 8736 Å EQUIVALENT WIDTHS IN LATE-TYPE GIANT AND SUPER-GIANT STARS

T. Merle[1], F. Thévenin[1], B. Pichon[1] and L. Bigot[1]

Abstract. Calcium and magnesium are key α-elements to study stellar populations in galaxies. Classical stellar abundances analyses rely on the local thermodynamic equilibrium (LTE) assumption which is not always appropriate, in particular for metal-poor and/or evolved stars. To better understand these stars and apprehend their impacts on the chemical enrichment of the Galaxy, it is necessary to use a Non-LTE (NLTE) description which is more realistic but also more complex to build up. For the calcium (Ca) and magnesium (Mg) lines in the RVS@Gaia, we computed theoretical NLTE corrections to apply to the measured equivalent widths of these lines using very complete model atoms of Mg and Ca. These corrections can be used by the automated abundance analysis methods based on equivalent widths for current and forthcoming large surveys.

Keywords: line: formation, radiative transfer, stars: abundances, stars: late-type

1 Why the Ca II IR triplet and the Mg I 8736 Å lines are important?

These lines are important because they represent lines of α-elements useful for derive abundances of magnesium, calcium and iron, and study the galactic enrichment. The IR ionized calcium triplet (CaT) is important since it allows us to determine the metallicity of red giant stars belonging to globular clusters (Armandroff & Da Costa 1991) and to dwarf spheroidal galaxies (Battaglia et al. 2008; Starkenburg et al. 2010) thanks to the measure of their equivalent widths at low resolution. The Mg I 8736 Å line is the only Mg I useful line at the resolution of the RVS[i]. It is a weak and unblended line not visible at metallicity lower than [Fe/H] ~ -2. Fig. 1 shows an example of spectra in the RVS (Radial Velocity Spectrometer) wavelength range for the Sun (integrated flux) where the CaT and the Mg I 8736 Å lines are labeled. Theoretical (red line) and observed (black line) spectra are compared at resolution of $R = 8500$. Theoretical LTE spectra is from MARCS model (Edwardsson, private communication) and observations are from Brault & Neckel (1987). The synthetic spectra reproduce well the observations except for few very weak lines for which the oscillator strengths are badly known and for the cores of the CaT which are formed in Non-LTE (NLTE) in the chromosphere, not included in the MARCS models.

2 How to compute line profile in Non-LTE?

As underlined by Asplund (2005), *"In non-LTE, in principle everything depends on everything else, everywhere else."*. This means that to compute line profile in NLTE, we need a huge amount of supplementary atomic data, concerning the element considered. In LTE, the line source function and the line opacity depend on the temperature, the free electron density and the LTE population number densities (governed by the Boltzmann and Saha's laws). In NLTE, the line source function and the line opacity depend on the NLTE population number densities of the element on which the line belongs, governed by the statistical equilibrium equations. To reach a better NLTE description a complete model atom in then required.

We used a modified version of the 1D NLTE radiative transfer code MULTI (Carlsson 1986). The radiative transfer and the statistical equilibrium equations are solve consistently using a theoretical MARCS model atmosphere (Gustafsson et al. 2008) for one element at a time. This element is considered as a trace element, i.e. is assumed to not disturb the structure of the model atmosphere. We constructed model atoms of Mg I and

[1] Laboratoire Lagrange, UMR7293, Université de Nice Sophia-Antipolis, CNRS, Observatoire de la Côte d'Azur, 06300 Nice, France
[i] whereas there is also a line at 8473 Å and a triplet at 8710, 8712 and 8717 Å.

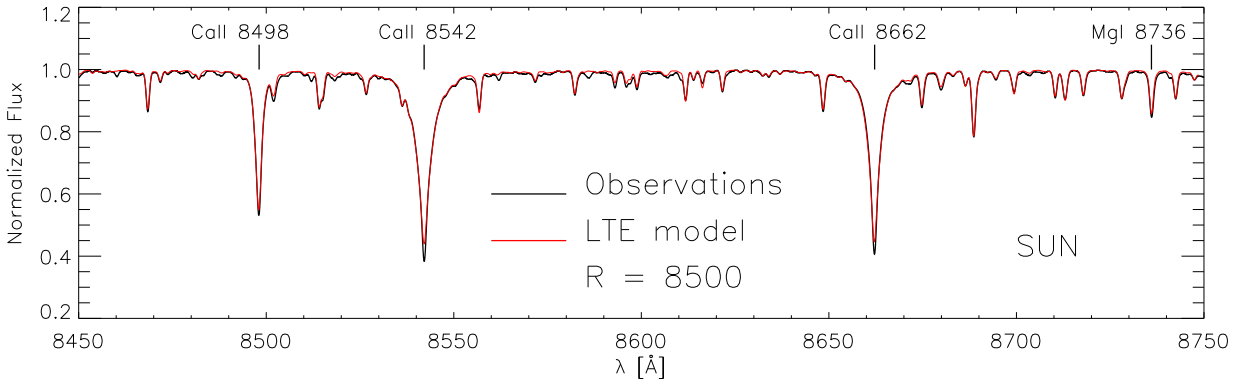

Fig. 1. Solar spectra in the RVS wavelength range.

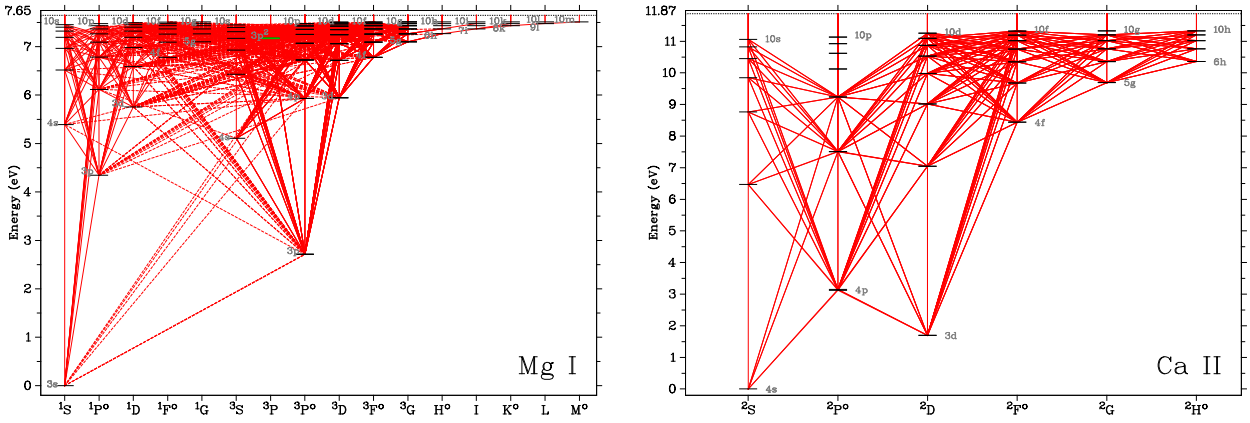

Fig. 2. Grotrian diagrams of Mg I (**left panel**) and Ca II (**right panel**). Solid red lines are the radiative transitions and dashed red lines (only for the Mg I model atom) are the semi-allowed transitions included in the models.

Ca II using the FORMATO code (Merle et al. 2011) which enables flexibility and modularity. Grotrian diagrams of model atoms of Mg I and Ca II are shown in Fig. 2. Energy levels until $n = 10$ are included. Fine structure is taken into account but not visible at this scale. The sources of atomic data are given in Merle et al. (2011). Oscillator strengths for the CaT are from Meléndez et al. (2007) and for Mg I 8736 Å line from VALD (Kupka et al. 2000). Inelastic collisions with neutral hydrogen were neglected since no reliable collision strengths with H were available until very recently for Mg I (Barklem et al. 2012).

3 What about the results?

We computed departure coefficients $b_i = n_i/n_i^*$ and NLTE/LTE equivalent width ratios W/W^* for a grid of atmospheric parameters:

- 3500 K $\leq T_{\rm eff} \leq$ 5500 K with a step of 200 or 250 K;
- $0.5 \leq \log g \leq 2.0$ with a step of 0.5 dex;
- $-4.0 \leq$ [Fe/H] $\leq +0.5$ with a step of 0.5 dex in $[-4.0, -1]$ and 0.25 in $[-1.0, +0.5]$;

for a galactic enrichment in α-elements (i.e. $[\alpha/\mathrm{Fe}] = 0.0$ in a metallicity range of $[0.0, +0.5]$, $[\alpha/\mathrm{Fe}] = -0.4[\mathrm{Fe/H}]$ in $[-1.0, 0.0]$ and $[\alpha/\mathrm{Fe}] = +0.4$ in $[-4.0, -1.0]$). The MARCS models with a mass of $M = 1 M_\odot$ and a constant microturbulent velocity fields of $\xi = 2$ km s^1 are adopted. We will discuss, hereafter, only the case of the CaT and the Mg I 8736 Å lines. Due to the importance of these lines for the Gaia mission, we computed

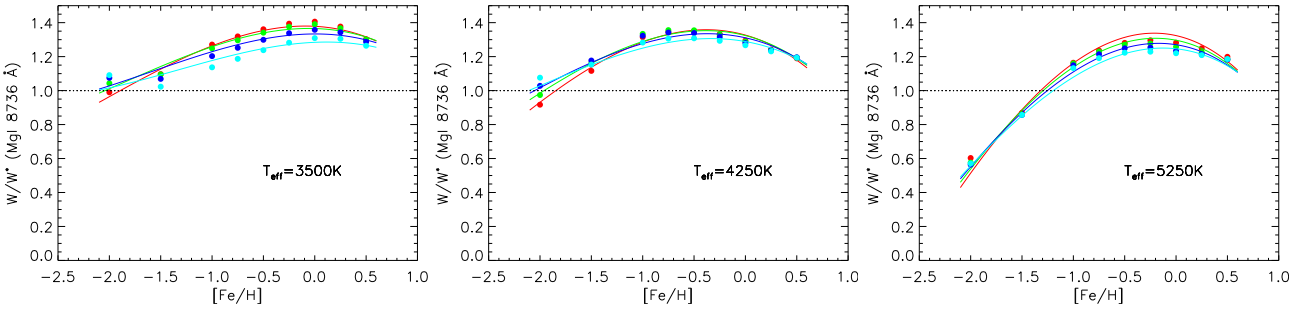

Fig. 3. W/W^* for the Mg I 8736 Å line as function of metallicity for three $T_{\rm eff}$. Each colour corresponds to a surface gravity (red, green, blue and cyan for $\log g = 0.5$, 1.0, 1.5 and 2.0 dex respectively). Dots represent theoretical results and full lines third order polynomial fits as a function of atmospheric parameters. The dotted line ($W/W^* = 1$) stands for no deviation from LTE.

fits of the W/W^* as a multivariable polynomial, using the LSQ package of Miller (1992). For each line of Mg I and Ca II in the RVS wavelength range, the W/W^* fit depends on $T_{\rm eff}$, $\log g$ and [Fe/H]. Theses fits can be used to estimate W/W^* with an accuracy better than 10 % in the range of stellar parameter considered. For more details on the other lines of these two α-elements see Merle et al. (2011).

The Mg I 8736 Å line, which is the most visible Mg I line in this RVS@Gaia range, is not visible under [Fe/H] ~ 2. Variations of W/W^* with atmospheric parameters are shown on the Fig. 3. Each panel represents the W/W^* of a given $T_{\rm eff}$ as a function of the metallicity [Fe/H]. Each colour represents a surface gravity (red, green, blue and cyan for $\log g = 0.5$, 1.0, 1.5 and 2.0 dex respectively). Dots are the computed values and full lines the polynomial fit. Its W/W^* is larger than one for a large range of stellar parameters and can reach $W/W^* = 1.4$ at solar metallicity. Positive values of W/W^* lead to a negative abundance correction, i.e., to an over-estimation of the Mg I abundance in LTE for this line. To our knowledge, there is only one previous study of the Mg I 8736 Å line in NLTE by Shimanskaya et al. (2000, and private communication). Their NLTE corrections for this line are lower due to the use of a semi-empirical formula to treat inelastic collisions with hydrogen.

The variation of W/W^* with [Fe/H] of the CaT (left panel of Fig. 4) can be explained with the variations of the departure coefficients presented in the right panel of Fig. 4. As the stimulated emission can be neglected for optical and near IR lines, the line source function relative to the Planck function S^l_ν/B_ν follows the departure coefficient ratio b_j/b_i (i and j are the lower and upper levels respectively). W/W^* depends on the values of b_i relative to b_j and on the deviation between them. In a metal-rich model (bold lines in right panel of Fig. 4), the levels are over-populated due to the over-ionization of Ca I and $b_i < b_j$ that implies $S^l_\nu > B_\nu$, and the emergent intensity is strengthened in the line compared to LTE intensity. Thus the EW in NLTE is lower than the EW in LTE. This explains why $W/W^* \leq 1$ for models with $-1 \leq$[Fe/H]$\leq +0.5$ in left panel of Fig. 4. For a metal-poor model (thin lines in right panel of Fig. 4), the mechanism is the opposite due to the change in the relative values of b_i and b_j. For metallicities lower than -1, $b_i > b_j$ if $\tau_{5000} \leq -1.7$ and then $S^l_\nu < B_\nu$. This implies a reduction of the emergent intensity in the line and then a larger value of EW in NLTE relative to the LTE. This explains why $W/W^* > 1$ for models with [Fe/H] ≤ -1 in left panel of Fig. 4.

The fine structure of the levels follows the same trends but level population differences increase with decreasing $\log \tau_{5000}$. The Ca II IR 8498 Å line has the greater NLTE effects relative to the two other lines because it has the largest amplitude on the deviation between the lower coefficient b_i ($3d\ ^2D_{3/2}$, blue dotted line) and the upper coefficient b_j ($4p\ ^2P^o_{3/2}$, red dashed line) as seen in right panel of Fig. 4. The CaT lines are dominated by their wings even at [Fe/H] $= -2$ as shown in fig. 1 of Starkenburg et al. (2010). These wings are formed in the deep photosphere in LTE conditions. Therefore the EW are weakly influenced by the NLTE effects at solar metallicity and can become very large for the most metal-poor stars (20-30% at [Fe/H] $= -3$). These results are in quite good agreement with those of previous investigations with the same stellar parameters (e.g. Jorgensen et al. 1992, Andretta et al. 2005).

We also compared the NLTE effects on CaT computed by Starkenburg et al. (2010) and found a clear discrepancy at low metallicity. They provided a 2D polynomial fit of $W^*/W = f(T_{\rm eff}, [{\rm Fe/H}])$ for the lines at 8542 Å and 8662 Å, considering that these ratios are insensitive to the surface gravity ($1 \leq \log g \leq 2$). We plotted in the left panel of Fig. 4 their polynomial fit for the 8662 Å line. The discrepancies between our

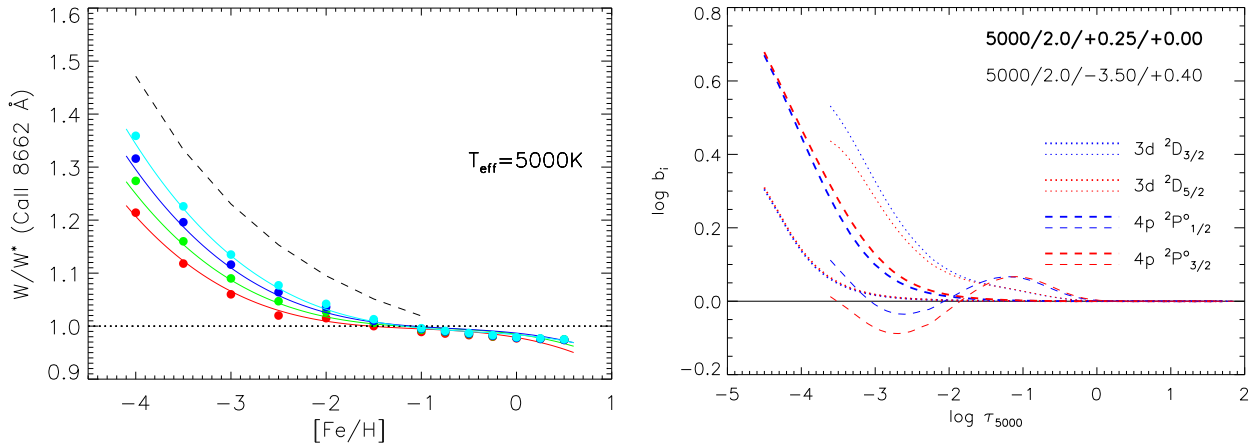

Fig. 4. Left: W/W^* for one of the component of the CaT at 8662 Å as function of metallicity. Colours have the same meaning than in Fig. 3. Dashed line represents the W/W^* fit obtained by Starkenburg et al. (2010). **Right:** Population number densities of the levels of Ca II involved in the CaT as a function of the radial optical depth in the continuum at 5000 Å $\log \tau_{5000}$ for a metal-rich (in bold) and a metal-poor model.

W/W^* and theirs, at a given $T_{\rm eff}$, increase with decreasing metallicity and with decreasing surface gravity. At [Fe/H] $= -4$, the deviation is about 10% for $\log g = 2$ and about 18% for $\log g = 1$. These differences may come from the fact that they used a different geometry (plane-parallel) in their study. We checked that the use of the scaling factor $S_H = 1$ for the collisions with neutral hydrogen cannot compensate this difference.

4 What can be learn from all of this?

We have performed NLTE computations for the Mg I and Ca II model atoms. We provide computed W/W^* for a grid of 453 MARCS model atmospheres of late-type giants and supergiants[ii]. The inclusion of fine structure in the model atoms do not affect strongly NLTE results since the W/W^* of the components of a multiplet are very similar but permit a consistent representation of the physics. The departures from LTE for the Mg I 8736 Å line are not negligible and must be taken into account to correctly estimate the magnesium abundance. The CaT lines are mainly formed in LTE if [Fe/H] ≥ -2. The NLTE effects increase with a decrease of the metallicity and with an increase of the surface gravity. We show that the W/W^*(CaT) can increase by 20% for $\log g$ varying from 0.5 to 2.0. In the context of large surveys as Gaia, the W/W^* tables and the polynomial fits (given in Merle et al. 2011) can be extensively used to remove the NLTE effects of the measured equivalent widths in the classical LTE abundance analysis using equivalent width fitting method.

References

Andretta, V., Busà, I., Gomez, M. T., & Terranegra, L. 2005, A&A, 430, 669
Armandroff, T. E. & Da Costa, G. S. 1991, AJ, 101, 1329
Asplund, M. 2005, ARA&A, 43, 481
Barklem, P. S., Belyaev, A. K., Spielfiedel, A., Guitou, M., & Feautrier, N. 2012, A&A, 541, A80
Battaglia, G., Irwin, M., Tolstoy, E., et al. 2008, MNRAS, 383, 183
Brault, J. & Neckel, H. 1987, ftp://ftp.hs.uni-hamburg.de/pub/outgoing/FTS-Atlas
Carlsson, M. 1986, Uppsala Astronomical Observatory Reports, 33
Gustafsson, B., Edvardsson, B., Eriksson, K., et al. 2008, A&A, 486, 951
Jorgensen, U. G., Carlsson, M., & Johnson, H. R. 1992, A&A, 254, 258
Kupka, F. G., Ryabchikova, T. A., Piskunov, N. E., Stempels, H. C., & Weiss, W. W. 2000, Baltic Astronomy, 9, 590
Meléndez, M., Bautista, M. A., & Badnell, N. R. 2007, A&A, 469, 1203

[ii] available on VizieR at CDS (J/MNRAS/418/863/grid) or upon request to the authors.

Merle, T., Thévenin, F., Pichon, B., & Bigot, L. 2011, MNRAS, 418, 863
Miller, A. J. 1992, Appl. Statist., 41, 458
Shimanskaya, N. N., Mashonkina, L. I., & Sakhibullin, N. A. 2000, Astronomy Reports, 44, 530
Starkenburg, E., Hill, V., Tolstoy, E., et al. 2010, A&A, 513, A34